

THE ELECTRIC FIELD AND WAVE EXPERIMENT FOR THE CLUSTER MISSION

G. GUSTAFSSON, R. BOSTRÖM, B. HOLBACK, G. HOLMGREN, A. LUNDGREN,
K. STASIEWICZ and L. ÅHLÉN

Swedish Institute of Space Physics, Uppsala Division, S-755 91 Uppsala, Sweden

F. S. MOZER, D. PANKOW, P. HARVEY, P. BERG and R. ULRICH

University of California, Berkeley, U.S.A.

A. PEDERSEN, R. SCHMIDT, A. BUTLER, A. W. C. FRANSEN, D. KLINGE and
M. THOMSEN

SSD/ESTEC, Noordwijk, The Netherlands

C.-G. FÄLTHAMMAR, P.-A. LINDQVIST and S. CHRISTENSON

Royal Institute of Technology, Stockholm, Sweden

J. HOLTET, B. LYBEKK and T. A. STEN

University of Oslo, Norway

P. TANSKANEN and K. LAPPALAINEN

University of Oulu, Finland

J. WYGANT

School of Physics and Astronomy, Minneapolis, U.S.A.

Abstract. The electric-field and wave experiment (EFW) on Cluster is designed to measure the electric-field and density fluctuations with sampling rates up to 36 000 samples s^{-1} . Langmuir probe sweeps can also be made to determine the electron density and temperature. The instrument has several important capabilities. These include (1) measurements of quasi-static electric fields of amplitudes up to 700 mV m^{-1} with high amplitude and time resolution, (2) measurements over short periods of time of up to five simultaneous waveforms (two electric signals and three magnetic signals from the search coil magnetometer sensors) of a bandwidth of 4 kHz with high time resolution, (3) measurements of density fluctuations in four points with high time resolution. Among the more interesting scientific objectives of the experiment are studies of nonlinear wave phenomena that result in acceleration of plasma as well as large- and small-scale interferometric measurements. By using four spacecraft for large-scale differential measurements and several Langmuir probes on one spacecraft for small-scale interferometry, it will be possible to study motion and shape of plasma structures on a wide range of spatial and temporal scales. This paper describes the primary scientific objectives of the EFW experiment and the technical capabilities of the instrument.

List of EFW PI and Co-Investigators (alphabetical order)

L. Blomberg², R. Boström¹, C. Cattell³, N. Cornilleau-Wehrin⁴, P. Decreau⁵,
A. Egeland⁶, C.-G. Fälthammar², R. Grard⁷, D. Gurnett⁸, G. Gustafsson¹ (PI),
C. Harvey⁹, B. Holback¹, G. Holmgren¹, Ø. Holter⁶, J. Holtet⁶, P. Kellogg³,
P. Kintner¹⁰, S. Klimov¹¹, J.-P. Lebreton⁷, P.-A. Lindqvist², R. Manning⁹, G. Marklund²,
N. Maynard¹², F. Mozer¹³, K. Mursula¹⁴, H. Opgenoorth¹, A. Pedersen⁷, H. Pecseli⁶,
R. Pfaff¹⁵, I. Roth¹³, A. Roux⁴, J. Singer¹⁶, R. Schmidt⁷, K. Stasiewicz¹,
P. Tanskanen¹⁴, M. Temerin¹³, E. Thrane¹⁷, L. Woolliscroft¹⁸, J. Wygant³.

Institutions

- ¹ Swedish Institute of Space Physics, Uppsala, Sweden.
- ² Division of Plasma Physics, Alfvén Laboratory, Stockholm, Sweden.
- ³ School of Physics and Astronomy, University of Minnesota, U.S.A.
- ⁴ CETP/USQV, Velizy, France
- ⁵ LPCE/CNRS, Orleans, France
- ⁶ University of Oslo, Oslo, Norway
- ⁷ Space Science Department/ESTEC, Noordwijk, The Netherlands
- ⁸ University of Iowa, Iowa City, Iowa, U.S.A.
- ⁹ DESPA, Meudon, France
- ¹⁰ School of Electrical Engineering Cornell University, Ithaca, New York, U.S.A.
- ¹¹ Space Research Institute Moscow, Russia
- ¹² Mission Research Corporation, Nashua, New Hampshire, U.S.A.
- ¹³ University of California, Berkeley, California, U.S.A.
- ¹⁴ University of Oulu, Oulu, Finland
- ¹⁵ Goddard Space Flight Center, Greenbelt, Maryland, U.S.A.
- ¹⁶ NOAA, Boulder, Colorado, U.S.A.
- ¹⁷ Norwegian Defence Research Establishment, Kjeller, Norway
- ¹⁸ University of Sheffield, Sheffield, England

1. Introduction

The Cluster mission of four identical spacecraft in nearby, non-coplanar orbits will for the first time give us measurements of magnetospheric structures in three dimensions and will improve the possibilities to separate between time and space variations.

The electric-field and plasma densities are essential quantities to measure in order to understand magnetospheric processes. The detailed high resolution measurements at each spacecraft combined with measurements of the large-scale gradient from the four spacecraft will be an important contribution to the mission.

Spherical double probes for measurements of electric-fields in magnetospheric plasma were first launched on the S3-3 spacecraft in 1976 (Mozer *et al.*, 1979) and has since then been used on a number of satellite missions. A review of the performance of double probes was given by Pedersen *et al.* (1984).

The four Cluster spacecraft will pass through numerous plasma regimes separated by different boundaries and discontinuities. This implies that the spacecraft will encounter a large variety of plasma phenomena at different scales both in time and space domain, as well as different field intensities. The EFW experiment has four spherical sensors located at the ends of 50 m long booms in the spin plane of the satellite. The electric-field component along the spin axis can only be constructed with the assumption that $\mathbf{E} \cdot \mathbf{B} = 0$. The experiment is well suited to study

both the large-scale structures, with four-spacecraft interferometry, as well as small (micro)-scale structures, with two (or more) probes operated in Langmuir mode on one spacecraft. Two analogue-to-digital converters can sample waveforms up to $36 \text{ ksamples s}^{-1}$ and can redirect the output to an internal (burst) memory of one Megabyte allowing sampling frequencies much higher than those permitted by the spacecraft telemetry system (i.e., $450 \text{ samples s}^{-1}$). To provide an adequate data base for studying physical phenomena in various magnetospheric regions, the electric-field and plasma fluctuation experiment is able to measure wave phenomena with temporal resolution of $110 \mu\text{s}$. This will cover wave frequencies from DC up to those of lower hybrid frequency and will make it possible to resolve small-scale electromagnetic structures. EFW will concentrate on taking full waveforms up to 180 Hz. Complementary electric and magnetic field data will be obtained by other experiments within the Wave Consortium (WEC). With interferometric (differential) timing between opposite probes the instrument will make it possible to measure small-scale plasma structures (viz., cavitons) and distinguish between spatial and temporal variations. This paper describes the primary scientific objectives of the experiment, its technical capabilities, and planned data-processing systems.

2. Scientific Objectives

2.1. ELECTRIC FIELDS AT SMALL SCALES

Some of the most interesting magnetospheric phenomena are associated with non-linear processes that result in the acceleration of plasma. Electric-field measurements on several satellites: S3-3, Viking, ISEE, and Freja have shown that particle acceleration is associated with large amplitude, short duration electric-field signatures. An example of a short duration (spiky) electric-field observed at bow shock is shown in Figure 2.1.

ISEE observations in the bow shock revealed intense, often bipolar, electric-field spikes with amplitudes of 100 mV m^{-1} and durations of 50 ms (Figure 1). It was not possible to fully determine the properties of these waves with the ISEE experiment but will be possible with Cluster. The phase velocities, scale size, polarisations relative to the ambient magnetic field, three-dimensional structures, coherence lengths, relation to comparable temporal scale density and magnetic-field fluctuations can be determined with the Cluster electric-field instrument. These quantities are needed to evaluate the role of the spikes in providing anomalous resistivity, thermalised ion and electron distributions, and in the production of high-energy electron beams commonly seen at the bow shock. Small localised plasma structures are inherently nonlinear and represent interesting objects for study both for fundamental plasma physics and for applied magnetospheric research. High-rate data sampling usually requires internal burst memory because of limits imposed by standard spacecraft telemetry. Whenever higher time resolution data have become

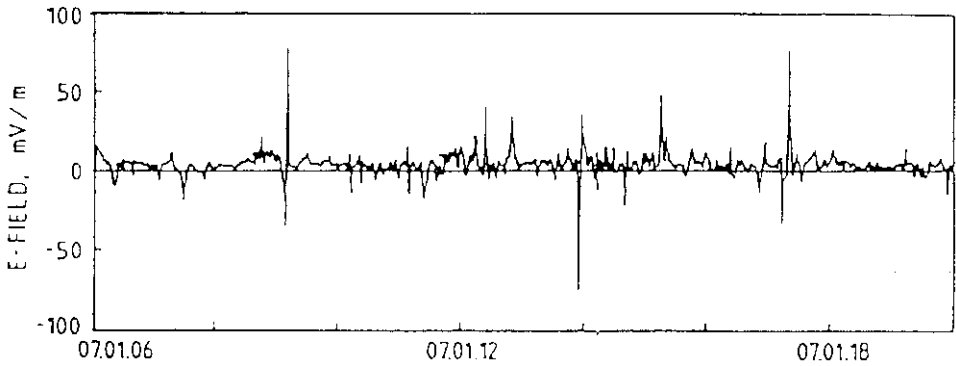


Figure 1. Measurements on ISEE-1 at 32 samples s^{-1} of spiky electric-field of 100 mV m^{-1} and a duration of 50 ms during bow shock crossing. This is a single-axis measurement, so the direction relative to the magnetic field is not known. On Cluster, the direction and phase velocity can be determined.

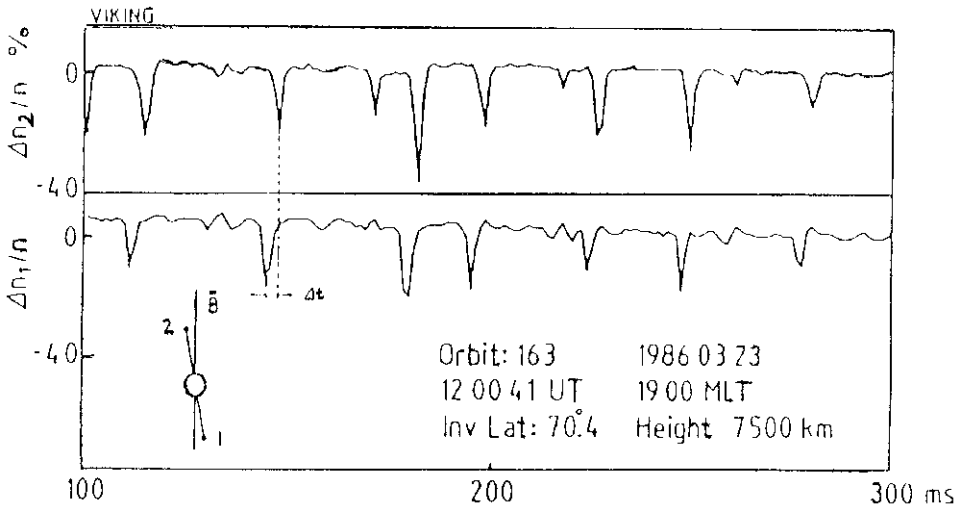


Figure 2. Weak double layers observed on Viking. These measurements show high time resolution recordings of density fluctuations on two Langmuir probes. From these data one can determine propagation velocity, scale length and net electric field (see Boström, 1988). Similar phenomena will be studied with Cluster in different regions of the magnetosphere.

available, new phenomena have been discovered. With the one Megabyte internal burst memory of EFW, it is expected that new phenomena will be observed requiring observations with high time resolution. An example is the observations of weak double layers on Viking shown in Figure 2.

The electric-field experiment and wave experiment on Freja (Marklund *et al.*, 1994; Holback *et al.*, 1994) provided many interesting observations on large-amplitude electric fields, plasma cavities associated with lower hybrid waves and large-amplitude modulated Langmuir waves in the auroral ionosphere (see special

issue *Geophys. Res. Letters* **21**, No. 17, 1994). We anticipate the discovery of similar and entirely new features in the high time resolution data to be obtained with the Cluster satellites at higher altitudes.

2.2. ELECTRIC FIELDS AT INTERMEDIATE SCALES

Many of the central scientific goals of the Cluster mission relate to electric fields at intermediate scales (hundreds of km to a few R_E). These include MHD turbulence in the solar wind, magneto-sheath and cusp, instabilities driven by velocity shears, waves associated with quasi-parallel shocks, flux transfer events, impulsive penetration of plasma into the magnetosphere, and slow mode shocks in the near tail in association with reconnection. Electric-field data will provide information which is vital for determining wave modes, wave vectors, phase velocities and energy flow. The spatial and temporal variation in the auroral zone electric-field is another interesting topic addressed by measurements on these spatial scales. Observations on several low-orbiting satellites have shown that discrete auroral arcs are associated with solitary kinetic Alfvén waves. The Cluster spacecraft will make it possible to search for and study possible magnetospheric footprints of solitary alfvénic waves. The average behaviour of the auroral zone electric-field and related electrodynamic parameters for various geophysical conditions is relatively well documented. This is, however, not the case for the ‘instantaneous’ auroral electro-dynamics on which very few studies have been conducted (Heelis *et al.*, 1983; Marklund *et al.*, 1986). A new technique to obtain global realistic and self-consistent distributions of auroral electrodynamic parameters has recently been developed (Marklund *et al.*, 1986). Simultaneous observations on the different spacecraft involved are used both for calibration of the model input data (field-aligned currents and conductivities) and for tests of the results (equipotential pattern). For these kinds of studies the Cluster mission with simultaneous four-point measurements will be ideally suited. The electric-field is an important parameter in studies of magnetohydrodynamic (MHD) turbulence. MHD turbulence is expected in all the important regions to be investigated by Cluster. The electric-field, together with the magnetic field, determines the Poynting flux and the propagation direction of the waves and plasma flows in these regions. The scale size and the magnitude of the electric fields involved have a wide range of values in these various regions. In the solar wind, scale sizes are several hundred kilometres to many thousands of kilometres and electric-field magnitudes are of the order of 1 mV m^{-1} . On auroral field lines, the electric-field is typically much larger. Magnitudes of over 100 mV m^{-1} are common and scale sizes from less than a kilometre to tens of kilometres. (Block *et al.*, 1987; Fälthammar *et al.*, 1987; Marklund *et al.*, 1987). The quasi-parallel shock structure provides a strong challenge to space physicists attempting to understand the role of different wave modes and scale sizes in the deceleration and thermalisation of upstream plasma. The four Cluster spacecraft can determine the phase velocity and Poynting flux of waves

and 'shocklets' upstream and downstream of the shock. In the absence of such measurements it has been difficult to distinguish between waves standing in the shock frame of reference, waves created in the upstream region and convected and amplified across the shock transition region, and waves created in the transition region.

2.3. ELECTRIC FIELDS AT LARGE SCALES

At the longest scale lengths of interest for the Cluster study are the electric fields associated with processes such as polar-cap-potential drop, convection in the 'quiet' magnetotail, and the formation of a near-Earth neutral line. Steady-state convection in the magnetotail has been examined using analytic and numerical methods as well as simulations (Erickson and Wolf, 1980). Their models will be tested for the first time using the Cluster electric-field data. Another aspect of large scale electric fields is the distinction between potential and inductive fields. ISEE-1 electric-field data have led to the suggestion that the electric fields associated with the hypothesised near-earth neutral line are confined to $\approx 10\text{--}15 R_E$ in the dawn-dusk direction (Cattell *et al.*, 1986; Pedersen *et al.*, 1984). Comparisons of observed electric fields in the tail ($20\text{--}40 \text{ mV m}^{-1}$ during candidate neutral line events) with cross-polar-cap potentials imply that the field is primarily inductive or associated with structures of limited size. The Cluster satellite electric and magnetic-field data will allow direct determination of associated electric fields, the relative importance of inductive and potential fields, as well as the relationship of the neutral-line-propagation speed to the electric field and where reconnection is initiated in the plasma sheet. The four satellites will also be able to determine the extent of substorm electric fields which may not be directly related to the neutral line (Pedersen *et al.*, 1985), in particular how these fields are related to substorm injection. Cluster electric-field data can provide additional, more detailed information for understanding plasma sheet motion, in particular, variations in the dawn-dusk and earthward-tailward directions. Multipoint measurements on Cluster will be complemented by ground-based observations of the ionospheric convection using the EISCAT/ESR facility on Svalbard, SuperDarn and other available ground facilities. These data will provide important information on the quality of magnetospheric models and equipotentiality of magnetic-field lines. We plan extensive use of software tools, developed by Stasiewicz (1994), for field line mapping of magnetospheric/ionospheric structures and visualisation of satellite orbits. The four-spacecraft configuration will make possible comprehensive investigations of the energy transfer by means of Poynting flux. The amount of electromagnetic energy that is converted to particle energy in a region is given by the integral of the flux over a closed surface bounding that region. It is important to note that it is not the Poynting flux but, rather, its integral over a closed surface, that is the physically meaningful quantity. Four-point simultaneous measurements of the Poynting flux on the four Cluster spacecraft can provide sufficient information to estimate the surface integral. When this surface encompasses

a physically interesting region such as the polar cusp, current sheet, magnetopause, etc., it should be possible to reach conclusions on whether acceleration processes or plasma heating are occurring at these locations.

3. Instrument Description

3.1. GENERAL

To meet the scientific objectives the electric-field instrument is capable of measuring, in various modes:

- Instantaneous spin plane components of the quasi-static electric-field vector, over a dynamic range of 0.3 to 700 mV m^{-1} , and with variable time resolution down to 0.1 ms .
- Oscillating electric-field in the range 50 – 8000 Hz and amplitude range 10 mV m^{-1} to $1 \mu\text{V m}^{-1}$.
- The thermal plasma density, over a dynamic range of 1 to 100 cm^{-3} .
- Plasma density fluctuations over a dynamic range of 1 to 50% with a time resolution of 0.1 ms .
- Time delays between signals from up to four different antenna elements on the same spacecraft, with a time resolution of $110 \mu\text{s}$.
- The spacecraft potential which can give information about electron density in the range 10^{-2} – 10 cm^{-3} with time resolution down to 0.2 s .

The sensor system of the instrument consists of four orthogonal cable booms carrying spherical sensors and deployed to 50 m in the spin plane of the spacecraft. Most of the electronics are contained in one electronics unit as shown in the block diagram in Figures 3 and 4.

The instrument has several important features. The potential difference between two opposite spherical sensors on orthogonal booms provides the average electric fields in two directions. The instrument can also operate the probes in Langmuir mode with voltage bias. By stepping the voltage bias the current-voltage characteristics of the plasma can be achieved to calculate the electron temperature and the plasma density. The output signals from the spherical sensor pre-amplifiers are made available to the other wave instruments for high-frequency wave measurements. The experiment has two fast Analogue-to-Digital, (A/D), conversion circuits for simultaneous sampling of two waveform signals at a rate of $36\,000 \text{ samples s}^{-1}$. At data rates above $450 \text{ samples s}^{-1}$, the data are buffered in a one Megabyte burst memory and played back through the ordinary telemetry stream in the playback mode. On-board least-square fit calculations of two components of the electric-field, averaged over one spacecraft spin period (4 s), will always be present in the telemetry stream, when two or more probes are operated in voltage mode. The measured signals are continuously monitored on board in order to detect conditions that are appropriate for triggering a burst collection of data.

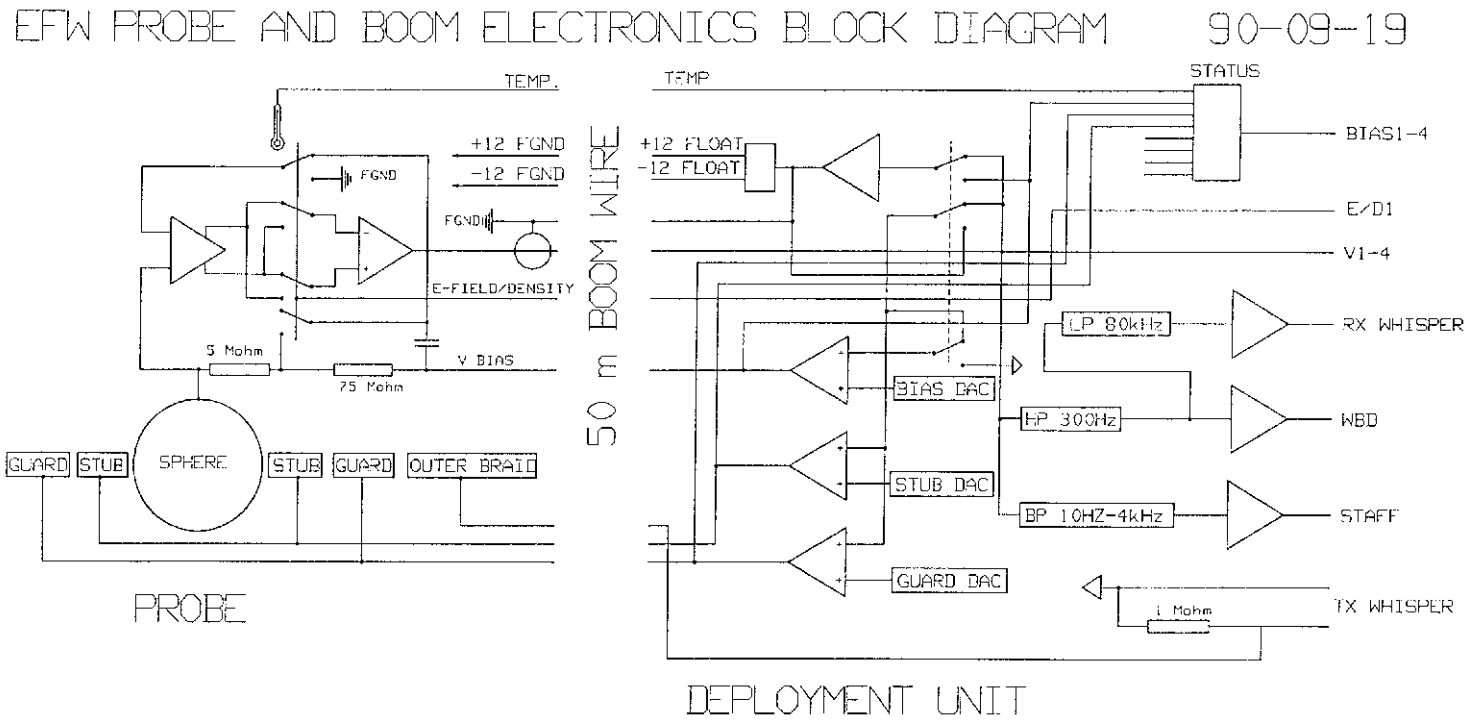


Figure 3. Block diagram of EFW.

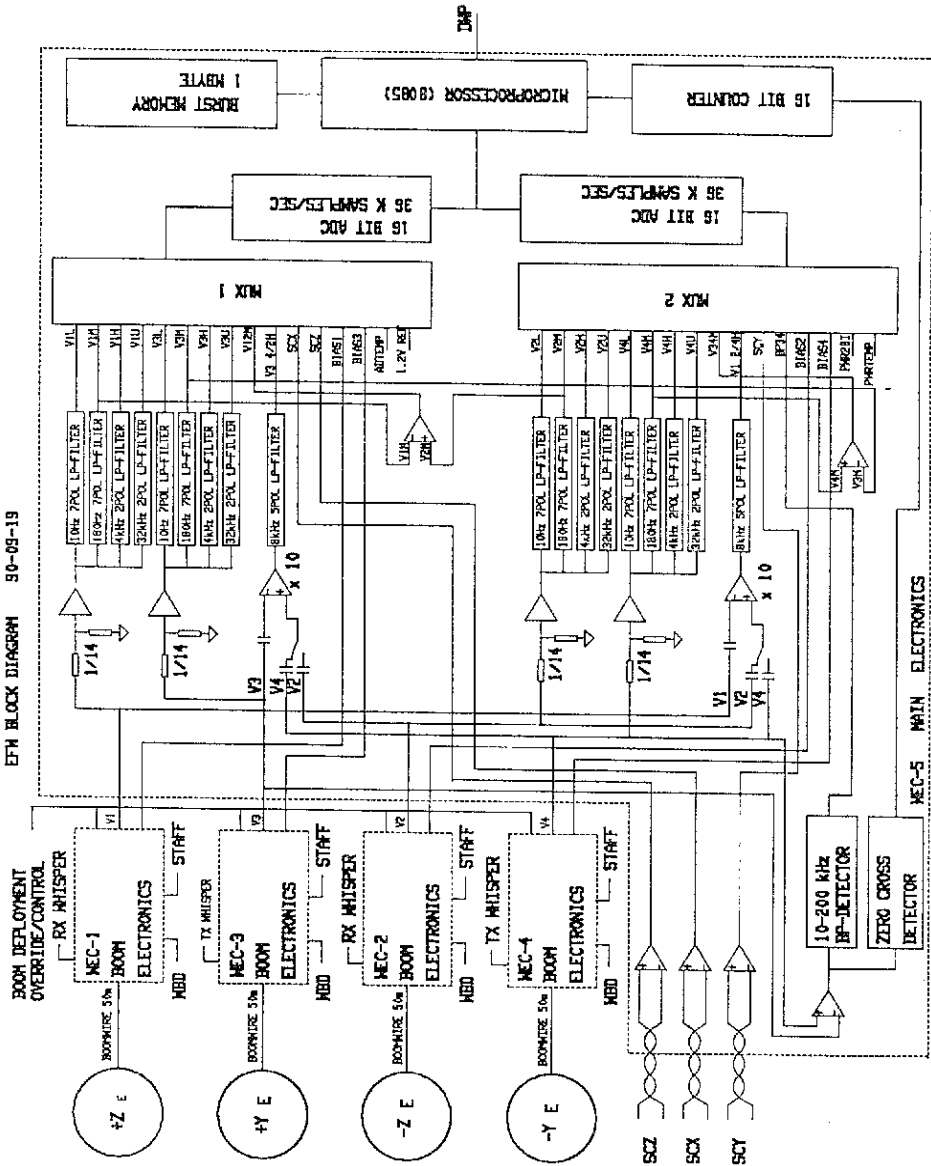


Figure 4. Block diagram of EFW.

Table I
Measured quantities

Quantity	Frequency	Range	Ampl. res.	Time res.
DC(E_y, E_z)	0–10 Hz	0.3 mV m ⁻¹ –700 mV m ⁻¹	22 μ V m ⁻¹	1/25 s
	0–180 Hz		22 μ V m ⁻¹	1/450 s
	0–4000 Hz		22 μ V m ⁻¹	1/9000 s
	0–32 000 Hz		22 μ V m ⁻¹	1/18 000
AC(E_y, E_z)	50–8000 Hz	1 μ V m ⁻¹ – 10 mV m ⁻¹	0.15 μ V m ⁻¹	1/18 000s
$n, \delta n$	0–10 Hz	1–100 cm ⁻³		1/25 s
	0–180 Hz			1/450 s
	0–4000 Hz			1/9000 s
n, T_e	DC	1–100 cm ⁻³ , eV range		
Freq. counter	10–200 kHz			

Table II
Data rates

Nominal mode data rate	1 440 bit s ⁻¹
Burst mode rates	15 040 bit s ⁻¹
	22 240 bit s ⁻¹
	29 440 bit s ⁻¹
Internal burst memory loading data rate	≤ 1152 kbit s ⁻¹

Characteristics of the instrument are shown in Tables I, II, and III. The search coil magnetometer data (not included in Table I) can also be routed through the 4 kHz channel of the EFW instrument.

3.2. WIRE BOOMS AND PROBES

Each of the four EFW boom units is a small, self-contained package containing two major components: a deployment mechanism and the multi-conductor cable with the spherical sensor. The mechanism design has evolved from a series of successful satellite experiments including S3-2 and S3-3, ISEE, Viking, Freja, CRRES and Polar. The deployment unit contains a rotating reel for the cable, a brush

Table III
Physical data

Item	Mass (kg)	Power (W)
Main electronics box	1.8	3.7
Wire booms 4 units	13.6	

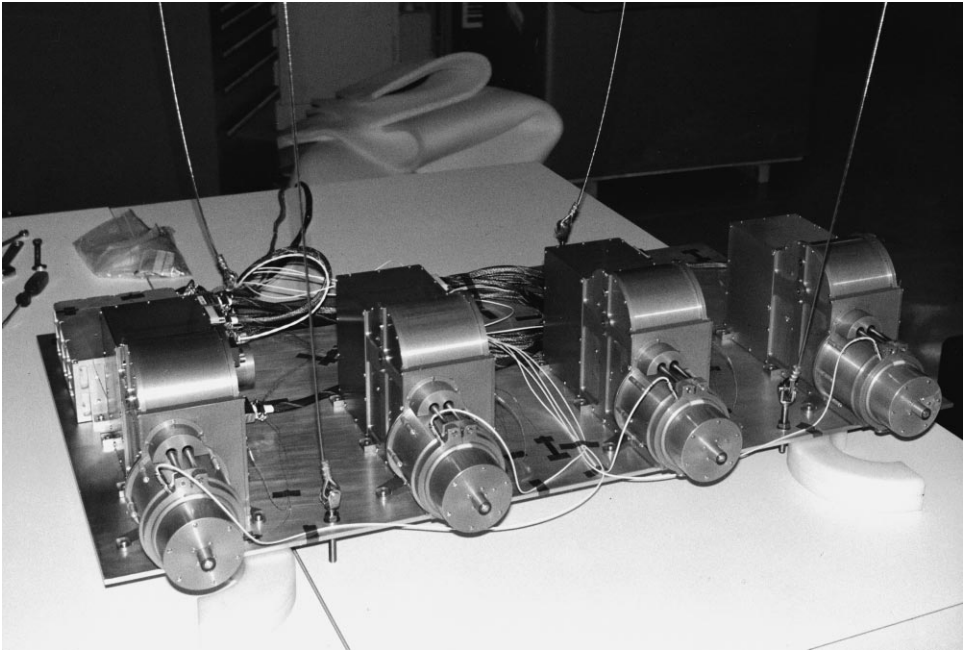


Figure 5. A picture showing the EFW instrument.

DC gear motor, an over-tension and end-of-cable indicator, an analogue cable-length indicator, a pyrotechnic-released spherical sensor housing, and a cable-oscillation Coulomb damper through which the cable exits the mechanism. In orbit, opposite booms will be symmetrically deployed to a probe-to-probe distance of approximately 100 m. However, the z -boom pair will be deployed to 70 m and kept at that length for about a week before being deployed to full length (100 m). A possibility for the satellite control to deploy the booms is also built into the system. The hardware elements of the experiment are shown in Figure 5.

The boom cable consists of eight wires and one coaxial cable, a kevlar braid that takes care of the mechanical stress due to the centrifugal force and, on top of it all, there is an outer braid made of conducting wire. The eight wires in the cable are used for power supply to the pre-amplifier housed in the sphere, for relay switching, for biasing voltages to the stub and guard, for probe temperature sensing and for biasing of the probe. The outer braid of one pair of booms is connected to the transmitter of the sounder experiment.

In order to limit (and control) the flux of photoelectrons from the boom wires to the spherical sensors and thereby minimise error sources, there is a special arrangement with the boom cable of symmetrical stubs and guards close to the probe. The outer braid is sectioned into stubs of 141 cm (from the probe surface) on both sides of the probe and the stubs are connected to guards of 10 cm length. Corresponding Stubs and a Guard are attached to the outer side of the probe for

symmetry reasons. The outer stub and guard wire is made similar to the boom wire and is wound on a reel in stowed configuration with a cover called Top Hat. When the centrifugal force exceeds a certain value during deployment of the boom, the Top Hat releases and the outer stub and guard wire stretches out. The outer stub and guard wire will cause a shadow effect on its 'own' probe that is similar to the shadow made by the boom wire on the opposite probe. This evens out asymmetries that otherwise would cause errors in the probe potentials.

The inner and outer stubs, hereafter only called the stub, are electrically connected to each other. Also the inner and outer guards, hereafter called the guard, are electrically connected. The stub and guard can be given different bias voltages in order to affect the flow of photoelectrons to and from the probe. The bias voltages are referred to the probe voltage and adjusted individually with an offset, one for each of the stubs and guards. The bias voltages are generated by 8 bit Digital-to-Analogue-Converters (DAC) located in the boom units. The stub voltage follows the sphere voltage with an offset which can be varied between ± 1.44 V in 256 steps. The guard voltage follows the sphere potential with an offset between ± 35.6 V in 256 steps.

The spheres are 8 cm in diameter and are made of aluminium. They are coated by electrically conducting paint containing graphite (DAG 213) which also provides a suitable temperature balance on the probes.

3.3. ANALOGUE ELECTRONICS

3.3.1. *Probe Modes*

There are two main modes of operation of the probes:

- The electric-field or voltage mode for potential measurement.
- The Langmuir or current mode for plasma density and temperature measurements.

In electric-field mode the pre-amplifier is set to high impedance input to allow the probe to adopt the potential of the surrounding plasma. In Langmuir mode the input impedance is low compared to the probe-to-plasma impedance so the probe can be given a bias potential and measure the resulting current. Switching between the two modes is achieved via a microprocessor-controlled relay in the probe and in the main electronics.

3.3.2. *Electric-field mode*

For the electric-field mode, the probe should be given a constant bias current. This is achieved by a voltage that is constant with respect to the probe potential over bias resistors. Thus, an offset voltage is added to the probe voltage and the resulting bias current can vary from -0.47 to $+0.47$ μA in 256 steps. Within these limits the bias current can be large enough to balance the maximum possible photoelectron flux to/from the spheres.

Each sphere is connected to the experiment electronics via a high impedance input pre-amplifier housed inside the sphere allowing the probe to adopt the potential of the surrounding plasma. Since the probe sheath has high resistance (10^7 – 10^{10} Ohms) and a capacitance of about 5 pF, the pre-amplifier must have high input impedance, low leakage current (<10 pA) and low input capacitance (<1 pF) to avoid attenuation of input signals. Since the potential of a biased sphere can differ from that of the spacecraft by 5–50 V in the absence of an electric-field, and fields as large as 500 mV m^{-1} have been observed, the dynamic range of the pre-amplifier and associated sensor electronics is ± 60 V from DC to 300 Hz. The small signal response exists to 600 kHz for use by other instruments on Cluster.

The sphere potential is determined by the balance of plasma electron current, photoemission current, and a bias current to the sphere. The magnitude of the bias current controls the ‘working point’ for the probe on the voltage-current characteristic curve and the aim is to find the working point that gives the lowest probe-to-plasma impedance.

3.3.3. *Langmuir Mode*

The spherical sensors can be operated as current-collecting Langmuir probes to provide information on the plasma density and electron temperature.

For this mode, the pre-amplifier in the probe is switched to low impedance input and the probe is given a bias voltage rather than a bias current as for the electric-field mode. The bias voltage is referred to satellite ground. Ideally, a positively biased probe collects an electron current that is proportional to the plasma density, provided the electron temperature is constant. Thus, variations in density will result in corresponding variations in the probe current. Also in this mode it is important to control the photoelectrons in order to minimise the errors that they cause.

3.4. DIGITAL ELECTRONICS

The digital electronics contains two fast, 16-bit, analogue-to-digital systems, a set of digital-to-analogue converters for biasing, a single 8-bit radiation-hardened microprocessor, and a one Megabyte burst memory. Extensive software functions increase the instrument’s capabilities and data coverage. The strategy for measuring the electric-field over a range of plus or minus 700 mV m^{-1} to a high relative accuracy can be achieved in a number of ways. With a 16-bit converter, the single-ended measurement of the sphere voltage (V1 through V4) will be possible from $22 \mu\text{V m}^{-1}$ to 700 mV m^{-1} . That gives a resolution of $22 \mu\text{V m}^{-1} \text{ bit}^{-1}$ over the whole range, but the noise level for DC measurements is expected to be about 0.1 to 0.3 mV m^{-1} due to photoelectrons from experience with previous missions. For AC measurements an additional gain of 148 times gives a range of 10 mV m^{-1} and a one-bit resolution of $0.15 \mu\text{V m}^{-1}$. The noise in this case corresponds to about $1 \mu\text{V m}^{-1}$.

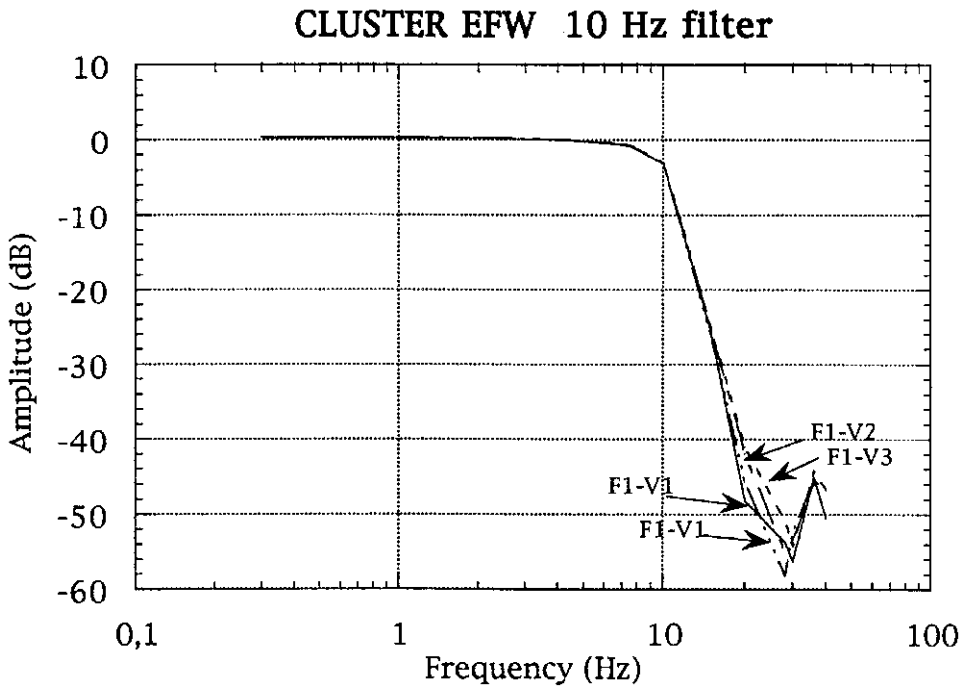


Figure 6. Instrument calibrations: frequency response of the 10 Hz filter.

3.5. INSTRUMENT CALIBRATION

An extensive series of amplitude, frequency response and phase calibrations were carried out at various stages of the integration of each of the instruments for the four satellites. The frequency response calibration was made for a large number of input amplitudes, DC offsets for each of the EFW filters. As an example we show the calibration of a 10 Hz and a 180 Hz filter, see Figures 6 and 7.

An example of a phase calibration is shown in Figure 8. A design goal has been to manufacture all the instruments as identically as possible. The calibrations made confirm that the instruments give similar results, so the calibration curves shown here are representative for all the instruments. Several calibrations will also be made after launch. Prior to boom deployment, small plasma simulators, included in the instruments, will be used to generate calibration signals. After deployment, the oscillating $\mathbf{V} \times \mathbf{B}$ electric-field signals generated by the spinning system will be used to compare the outputs from the four probes on each satellite. This is a high accuracy test if made in areas of space with constant plasma parameters for the time duration of one spin. Finally, in regions of space where plasma parameters can be assumed to be constant over large areas of space, a comparison can be made between instruments on the four spacecraft. Other methods that can be used for in-flight calibrations are statistical studies and measurements from other instruments.

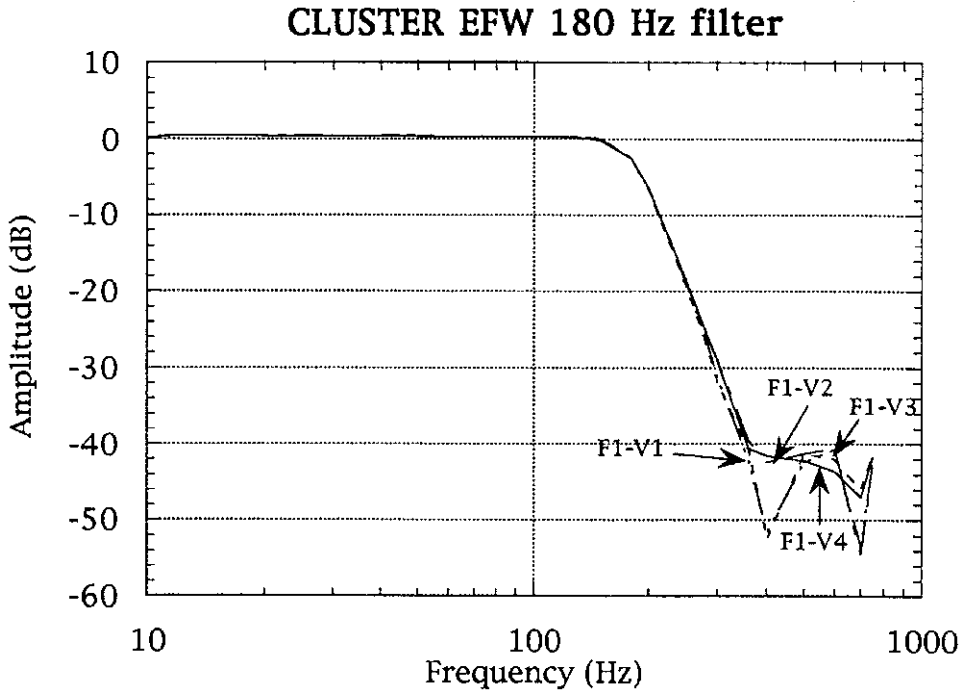


Figure 7. Instrument calibrations: frequency response of the 180 Hz filter.

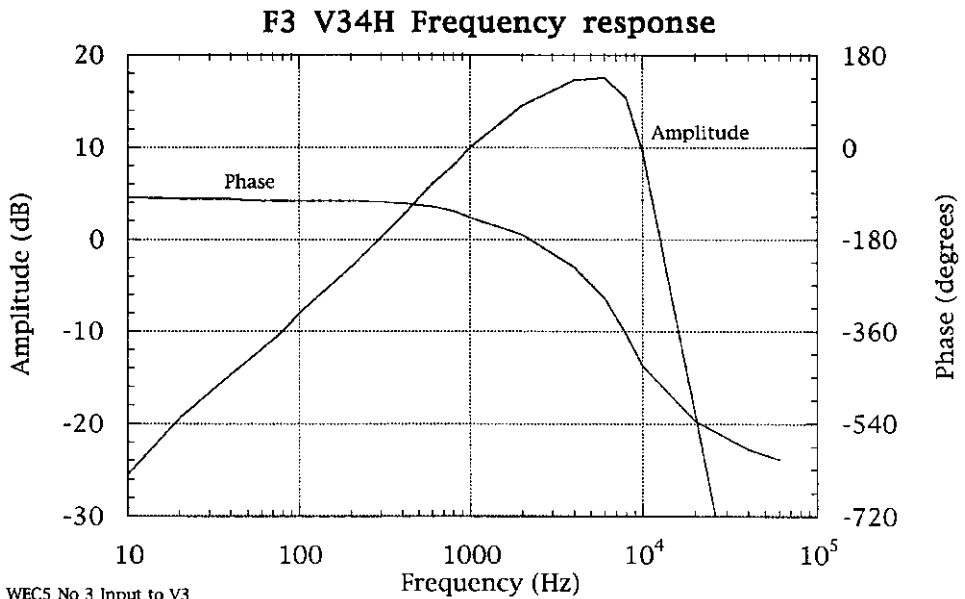


Figure 8. Instrument calibrations: an example of phase and amplitude response of the instrument.

3.6. EFW OPERATIONAL MODES

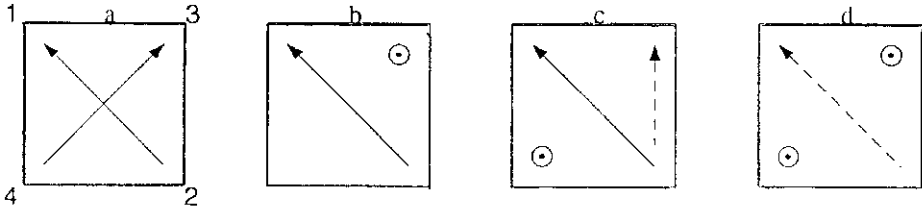
The EFW instrument has a large number of possible sampling modes. The main parameters to be selected in each case are: probe bias, probe mode, filter frequency, data rate and internal memory use. Several of the parameters are interrelated which limits the possible number of combinations, the telemetry rate is also dependent on other instruments in the WEC. The main combinations of probes and data rates are shown schematically in Figure 9.

The four probes can all be operated individually in current mode (to measure density/temperature), or voltage mode (to measure electric field) (see Figure 9). In some combinations voltages are measured from probe to satellite and in some cases differentially between two probes. The three components from the search coil instrument are also available in EFW with a bandwidth of 4 kHz. A diagnostic sweep, of 1–2 s duration, is performed approximately every 30 min. A bit in the EFW telemetry will indicate the occurrence of the sweep. Each probe signal is transferred through an anti-aliasing filter and sampled by one of the two A/D converters. Low pass filters at 10 Hz, 180 Hz, 4 kHz, or about 32 kHz, or a bandpass filter for 50 Hz to 8 kHz are available. The low telemetry rate (normal mode) limits the direct transmission to 10 Hz ($25 \text{ samples s}^{-1}$) but for the high telemetry rate (burst mode) 180 Hz ($450 \text{ samples s}^{-1}$) can be obtained. Frequencies above that may be recorded with the internal burst memory. There is also a simple frequency counter and an rms detector for 10–200 kHz available to detect the plasma frequency. The data transfer from EFW to telemetry goes via the Digital wave processor instrument (DWP) and can be made at four different rates: 1440, 15 040, 22 240, or 29 440 bit s^{-1} . All data rates contain 640 bits of housekeeping data (except for a few very exceptional cases) and in addition $2 \times 25 \text{ samples s}^{-1}$ of data, e.g., voltage differences between two pairs of probes for the 1440 bit s^{-1} case; $2 \times 450 \text{ samples s}^{-1}$ of data, e.g., voltage difference between two pairs of probes for 15 040 bit s^{-1} ; $3 \times 450 \text{ samples s}^{-1}$ of data, e.g., voltage difference between one pair of probes and currents from two probes for 22 240 bit s^{-1} ; and finally $4 \times 450 \text{ samples s}^{-1}$ of data, e.g., currents from four probes for the data rate of 29 440 bit s^{-1} . These and more combinations for each of the EFW data rates are shown in Figure 9. Each square of the figure shows one combination of probes for a particular data transmission rate, shown as one row. As an example, mode EFW1a corresponds to two perpendicular vector measurements of the electric-field, in the spin plane, giving a total data rate of 1440 bit s^{-1} . After gaining experience with the instrument in orbit the number of combinations may be reduced. There is also a possibility, not shown in Figure 9, to measure two parallel electric-field vectors separated in space in, e.g., mode EFW2a. EFW carries out on-board estimates of the spacecraft potential that are sent to DWP for distribution to other instruments. For this calculation at least two probes operated in the voltage mode are required, which is not the case when three or four probes are operated in current mode. EFW also has the capability to make on board preliminary estimates of the DC electric-

EFW PROBE CONFIGURATION

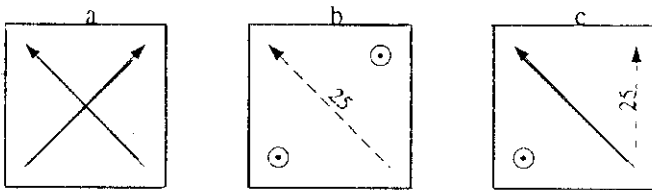
TM MODE EFW 1 1440 bits/s

Signals sampled at 25 samples/s



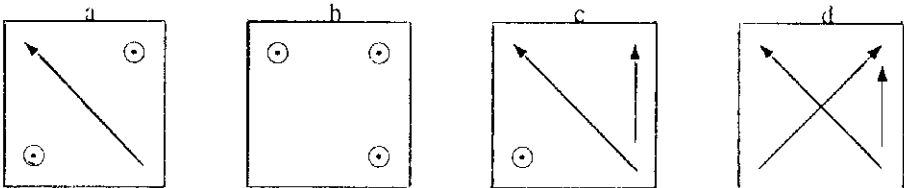
TM MODE EFW 2 15040 bits/s

Signals sampled at 450 samples/s unless otherwise noted



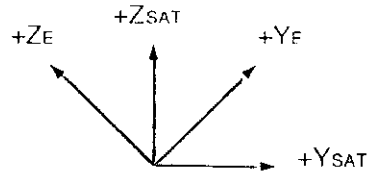
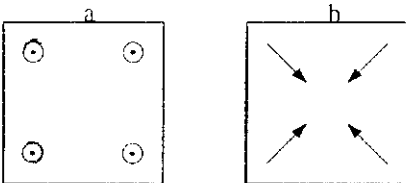
TM MODE EFW 3 22240 bits/s

Signals sampled at 450 samples/s



TM MODE EFW 4 29440 bits/s

Signals sampled at 450 samples/s



⊙ current mode

→ voltage mode

WHISPER Tx on YE

WHISPER Rx on ZE

Figure 9. The software and hardware has been made to accommodate the probe combinations shown in each box in the figure. The broken lines indicate that these modes imply some compromise regarding the content of the telemetry format to get sufficient space.

field by means of spin fit calculations. The EFW internal memory storage will be used to register signals from the filters with frequencies 0–4 kHz, 50 Hz to 8 kHz and 0–32 kHz, as data from these frequencies cannot be transmitted in real time due to telemetry limitations. The 4, 8, and 32 kHz signals are sampled at 9, 18 and 36 ksamples s^{-1} , respectively, and stored in the internal memory. The triggering of the internal memory can be made by ground commands, or by an internal algorithm based on EFW data, search coil magnetometer data or on fluxgate magnetometer data via DWP or an event flag from the fluxgate magnetometer.

3.7. DATA HANDLING AND TELEMETRY

3.7.1. *Telemetry description*

The EFW instrument sends scientific and housekeeping data to DWP for packaging and telemetry of the data. The telemetry contains 16-bit measurements of currents or voltages. The housekeeping data contains; on-board calculation of the electric-field, where the electric-field, in the spin plane, is measured at 32 equidistant angles and a least squares sine fit is made to obtain the field, housekeeping parameters about the instrument every 0.2 s and finally low rate data of voltages sampled at 5 samples s^{-1} . A special telemetry mode (called BM3) is available where the internal burst memory can be emptied in 6 min. Dumps are also possible in the modes called BM2 and BM3. Parts of the memory may also be emptied at a very low rate through the regular telemetry modes.

3.7.2. *On-Board Data Handling*

The Cluster EFW instrument communicates with DWP by a single 38.4 kbit s^{-1} serial link. EFW accepts commands, telemetry codes and fluxgate magnetometer data (8 vectors s^{-1}) from the DWP unit, and transmits telemetry data to DWP. The EFW software coordinates real-time sampling along with Internal Burst (high sampling rate) data collections. The total A/D rate is 36 000 sample-pairs per second. EFW software must allocate samples out of this total collection rate between real-time samples, burst samples, boom monitoring, sweep collection points, etc. The user controls how many of the samples may be used for real-time and non-burst versus how many can be used in bursts.

3.7.3. *Scientific Data Handling*

A major effort has been spent on software development in preparation for the EFW scientific data analysis. Two major software packages have been developed: the Orbit Visualisation Tool (OVT) and the Interactive Science data Analysis Tool (ISDAT). They are both general, not project specific, tools, implying that they can be utilised for any similar project and facilitate an inter-project and inter-instrument analysis of the data. In addition, the EFW team has actively contributed to the Cluster Science Data System (CSDS).

Table IV
EFW CSDS parameters

Parameter	Units
Duskward electric-field	mV m^{-1}
Standard deviation of E-dusk	mV m^{-1}
Electric-field power 1–10 Hz	$(\text{mV m}^{-1})^2 \text{ Hz}^{-1}$
Electric-field power 10–180 Hz	$(\text{mV m}^{-1})^2 \text{ Hz}^{-1}$
Probe current	A
Probe-spacecraft voltage	V

The Orbit Visualisation Tool (OVT)

The OVT is a versatile interactive graphical tool by which the user can:

- Visualise single or multi-spacecraft positions and orbit predictions.
- Relate the spacecraft position to magnetic-field models.
- Trace magnetic-field lines.
- Visualise magnetic iso-surfaces and borders.
- Visualise experimental data in magnetospheric model frames.

The Interactive Science Data Analysis Tool (ISDAT)

The ISDAT is a general-purpose tool that facilitates science data access in a uniform way locally or over networks. It is based on a client server architecture with a well-defined general data structure for the communications between the server and the clients. The system provides a limited number of data analysis and visualisation tools but, more importantly, allows the user to easily add on his own data analysis and display clients. The ISDAT has been adopted as the common tool for WEC scientific data analysis and it also constitutes an integral part of the CSDS User Interface. Hereby, for the EFW and WEC, full resolution data analysis can be combined with access to lower resolution data from other instruments provided by the CSDS (see also Pedersen *et al.*, this issue, for a more detailed description of the WEC data analysis plans).

The Cluster Science Data System (CSDS)

The CSDS is a Cluster project-wide effort to provide Cluster scientific data to a wide scientific community (see Schmidt *et al.*, this issue). The EFW CSDS parameters are produced at the CSDS Scandinavian Data Centre, Alfvén Laboratory, Royal Institute of Technology, Stockholm. The EFW parameters provided by CSDS are listed in Table IV.

Acknowledgements

The funding of the instruments was provided in Sweden by Swedish National Space Board; in U.S.A. by NASA; at ESTEC from ESA; in Norway by the University of Oslo; in Finland by University of Oulu and the Academy of Finland.

The design and fabrication of the instrument was a cooperative effort by several laboratories under management by the Swedish Institute of Space Physics in Uppsala. The following laboratories have contributed to hardware, software and/or ground support instruments: Space Science Laboratory at Berkeley, Space Science Department of ESTEC, Alfvén Laboratory in Stockholm, University of Oslo and University of Oulu. We would like to thank Anita Rogelius and Gunny Janzon at IRF-Uppsala for assistance with administration of the project.

References

- Block, L. P., Fälthammar, C. G., Lindqvist, P.-A., Marklund, G., Mozer, F. S., and Pedersen, A.: 1987, *Geophys. Res. Letters* **14**, 435.
- Boström, R., Gustafsson, G., Holback, B., Holmgren, G., Koskinen, H., and Kintner, P.: 1988, *Phys. Rev. Letters* **61**, 82.
- Cattell, C. A., Mozer, F. S., Jr., Hones, E. W., Anderson, R. R., and Sharp, R. D.: 1986, *J. Geophys. Res.* **91**, 5663.
- Erickson, G. M. and Wolf, R. A.: 1980, *Geophys. Res. Letters* **7**, 900.
- Eriksson, A. and Boström, R.: 1995, Irf Scientific Report 220. Technical Report, Swedish Inst. of Space Phys., Uppsala.
- Fälthammar, C. G., Block, L. P., Lindqvist, P.-A., Marklund, G., Pedersen, A., and Mozer, F. S.: 1987, *Ann. Geophys.* **5**, 4.
- Gustafsson, G. *et al.*: 1993, in R. Schmidt (ed.), *Cluster: Mission, Payload and Supporting Activities*, ESA SP-1159, p. 17.
- Heelis, R. A., Foster, J. C., de la Beaujardière, O., and Holt, J.: 1983, *J. Geophys. Res.* **88**, 111.
- Hilgers, A., Holback, B., Holmgren, G., and Boström, R.: 1992, *J. Geophys. Res.* **97**, 8631.
- Holback, B., Jansson, S.-E., Åhlén, L., Lundgren, G., Lyndgal, L., and Powell, S.: 1994, *Space Sci. Rev.* **70**, 577.
- Marklund, G. T., Heelis, R. A., and Winningham, J. D.: 1986, *Can. J. Phys.* **64**, 1417.
- Marklund, G. T., Blomberg, L. G., Potemra, T. A., Murphree, J. S., Rich, F. J., and Stasiewicz, K.: 1987, *Geophys. Res. Letters* **14**, 329.
- Marklund, G., Blomberg, L., Lindqvist, P. A., Fälthammar, C.-G., Haerendel, G., Mozer, F., Pedersen, A., and Tanskanen, P.: 1994, *Space Sci. Rev.* **70**, 483.
- Mozer, F. S., Cattell, C. A., Temerin, M., Torbert, R. B., von Glinski, S., Woldorff, M., and Wygant, J.: 1979, *J. Geophys. Res.*, **84**, 5875.
- Pedersen, A., Cattell, C. A., Fälthammar, C. G., Formisano, V., Lindqvist, P.-A., Mozer, F. S., and Torbert, R. B.: 1984, *Space Sci. Rev.* **37**, 269.
- Pedersen, P., Cattell, C. A., Fälthammar, C.-G., Knott, K., Lindqvist, P. A., Manka, R. H., and Mozer, F. S.: 1985, *J. Geophys. Res.* **90**, 1231.
- Schindler, R. and Birn, J.: 1982, *J. Geophys. Res.* **87**, 2263.
- Stasiewicz, K.: 1994, in A. Egeland, J. Holtet, and P. E. Sandholt (eds.), *Physical Signatures of Magnetospheric Boundary Layers*, Kluwer Academic Publishers, Dordrecht, Holland, p. 433.